CHAPTER VII

Synthesis, Characterization and Innovative Applications in Pharmaceutical Sciences of 2:1 Host Guest Inclusion Complexes assembled of Cyclic Oligo-Saccharides with Antispasmodics

Abstract: Solubility development of supramolecular host-guest interaction between Alverine citrate with αand β-cyclodextrins were studied throughout the article. 2:1 host to guest stoichiometry of the inclusion complexation in the solution phase were confirmed by the Job's plot and further confirmation about the stoichiometry was also obtained from the mass spectra of the inclusion complexes. IR, DSC, SEM and PXRD data turn out to be supportive about the phenomenon, inclusion complexation. Association constants and thermodynamic parameters of the inclusion complexes were obtained using UV-vis and spectrofluorometric measurement. The mechanism of inclusion complexation was explored by 1H and 2D ROESY NMR spectroscopy. Binding ability of the drug molecule, Alverine citrate with the HSA and the controlled release of the drug molecule from inclusion complexes were studied at PH-7.4 by spectrofluorimetricaly. Studied phenomenon thus develops the solubility of merely soluble drug into water, consequently makes bioavailable and enriches the drug delivery system.

Keywords: Alverine citrate; HSA; Controlled Drug delivery; Inclusion Complex; Solubility enhancement

1.Introduction:

Irritable bowel syndrome (IBS), a gastrointestinal disorder is a most commonly diagnosed gastroenterological problem in medical sciences. Patients suffering from IBS are found to suffer frequently from various gastrointestinal disorder like, abdominal pain or dis-comfort, altered bowel habit, bloating[1,2] associated with the symptoms, incomplete bowel movement, urgency and tenesmus[3, 4]. Thus, irritable bowel syndrome is a functional gastrointestinal disorder showing a lot of

abnormalities. Hyper-reactive intestinal motility[5] and visceral hypersensitivity are also found in patients suffering from IBS.

Alverine citrate (ALVC) **(Scheme 1)** belonging from a class of antispasmodic drugs used to treat irritable bowel syndrome and diverticular disease. Alverine citrate acts as a muscle relaxant and relieves abdominal pain, constipation or diarrhoea caused by the abnormal activity of the gut muscle. It also relaxes the muscle in the womb which is caused by the muscle spasms in uterus. Voltage-gated calcium channels are the main transducers of membrane potential changes into intracellular Ca^{2+} transients such a way they intervene smooth muscle contraction and activate endocrine to release hormone[6, 7, 8]. The visceral pronociceptive effect of 5-HTcan be reduced as ALVC binds with 5-HT1A acting as an antagonist. ALVC when combined with simethicone, found to act more effectively in the treatment of abdominal pain in IBS. It is marketed commercially by the name Spasmonal® Forte in the form of hard capsule (Alverine citrate 60/120 mg) and soft capsule (60 mg Alverine citrate/300 mg simethicone). ALVC ultimately metabolised to two secondary metabolites through the conversion of its primary active metabolite, para hydroxy alverine (PHA)[9].

The supramolecular interaction between ALVC and cyclodextrins (CDs) to form inclusion complex was justified satisfactorily by the improvement of two novel aspects - (a) solubility of the ALVC into water for bioavailability, (b) drug delivery through HSA assisted controlled release from inclusion complexes.

A drug to show greater therapeutic effectiveness needs its bioavailability and solubility to a large scale. Pharmacological response to be shown by a drug a minimum concentration of it must be achieved, in this connection aqueous solubility of the drug to a desired level is significant. Solubility of a molecule may be defined qualitatively as the spontaneous interaction of two or more substances to form a homogeneous molecular dispersion. It is found that ALVC-CDs inclusion complexes enhances the aqueous solubility of drug making it more bioavailable. Encapsulation of the hydrophobic part of the guest (ALVC) molecule into the hydrophobic cavity of suitable dimension of CDs makes it to increase aqueous solubility. The cavity dimension of the CDs should be moderate to reduce the contact between water and the nonpolar regions of host and guest molecule. Among the CDs, α and β-

cyclodextrins were used for the dimensional suitability of their cavity size **(Scheme 1)**.

As the organism – environment interaction is essential for its survival, on the molecular level small molecule like drug – protein/drug – gene product interaction is also essential that underlie the organism's ability to adapt to environmental changes and include those that bind, transport, and metabolize small molecules. Human serum albumin, the most abundant protein in blood plasma found to act as a carrier protein for vitamin, nutrients, hormone, steroid, drug like small molecule of low water solubility and binding ability of these molecules to HSA constitute a vibrant matter in pharmacokinetics[10, 11, 12, 13]. Here, binding property of ALVC to the HSA had been studied spectrofluorimetrically. Thus, HSA assists the drug ALVC to release from the inclusion complexes and makes its transportation to the affective area where adsorption of the drug molecule to be needed. Our study to form inclusion complexes of ALVC thus become moralised by the solubility enhancement and HSA assisted transformation and controlled release of the drug in human body.

2. EXPERIMENTAL SECTION

2.1. Materials

Alverine citrate, α and β-cyclodextrin, purity ≥98.0% and ≥97.0% were purchased from Sigma-Aldrich and were conserved in a refrigerator as received.

2.2. Apparatus

The Agilent 8453 UV-Visible Spectrophotometer was performed to record UV-vis spectra with an uncertainty of wavelength accuracy of ±0.5 nm. An automated digital thermostat, Julabo was used to control the cell temperature during experiments.

HRMS spectra of the solid ICs were recorded on a quadrupole time-of-flight (Q-TOF) high-resolution instrument with positive-mode electrospray ionization taking the methanol solution of the solid ICs.

2D ROESY as well as 1H NMR spectra were recorded in D_2O solvent at 400 MHz in Bruker Avance instrument at 298.15 K. The chemical shifts data, δ values are

presented in parts per million where, the residual protonated signal (HDO, δ 4.79 ppm) was used as internal standard.

With the help of Perkin-Elmer FTIR spectrometer the FTIR spectra of the solid ICs as well as the pure compounds were recorded in the scanning range of 4000−400 cm^{-1}at room temperature. KBr disk of the samples were prepared in the suitable ratio of sample to KBr to minimise noise.

Powdered X-Ray Diffraction (PXRD) patterns of the pure compound and ProC were recorded by using Cu-Kαradiation (D8 Advance Bruker)

The DSC thermograms of the samples were recorded with the help of Perkin-Elmer DSC-6 differential scanning calorimeter at the heating rates of 10°C min^{-1}. The thermograms were taken by heating near about 1 mg of samples in aluminium crimped pans under nitrogen gas flow.

The Scanning Electron Microscope (SEM), JEOL JSM IT 100 was used to determine the surface topography of the samples at various resolutions. Samples were prepared on a small piece of double adhesive carbon-coated tape attached to brass stubs and then a coating of ultra-thin layer of gold ions was put in a gold-ionization chamber.

The Bench top spectrofluorimeter from photon technologies International (Quantamaster-40, USA) was used to record fluorescence spectra at room temperature. Hellma quartz cuvette having optical path length 1.0 cm was also used.

2.3. Procedure

Solubility of ALVC and CDs were checked and the solutions were prepared with triply distilled water. A digital analytical balance METTLER TOLEDO AG-285 was used weigh with an uncertainty of ±0.1 mg taking sufficient precautions to avoid loss of materials. The aqueous solution of ALVC and CDs were prepared separately in the same molarity. The aqueous solution of CDs in a beaker then placed on a hot top of a magnetic stirrer for stirring. After that, aqueous ALVC solution was added dropwise to the solution of CDs placed on magnetic stirrer and the equimolar mixture of ALVC and CD solutions were allowed to stir for 8 hours keeping temperature at 40-45°C.

The suspensions obtained after cooling the mixture to 5 °C were filtered to obtain white crystalline powder, which were then dried in air and preserved in vacuum desiccators.

3. Result and discussion

3.1 Job plot: Stoichiometry of inter molecular association between guest and host:

According to the well-established Job's method the stoichiometry of the host-guest inclusion complexes was determined using the UV-vis spectroscopic data[14, 15]. A set of solutions in the range of 0 – 1 mole fraction were prepared by mixing aqueous ALVC and CDs in the calculated proportion and recorded the spectra at 298.15 K of temperature. Absorbances of the set of solutions at λ_{max} = 258 nm were considered for the calculation to obtain the Job's plot **(Figure 1).** Plotting ΔA×R vs R generates the Job's plot and value of R corresponding to the maxima of Job's plot signifies the stoichiometry of inclusion complexes. Where, ΔA represents the differences in absorbance between pure ALVC and each of the solutions of the set **(Table S1, S2 and Figure 1)**. R indicates [CDs]/[ALVC]+[CDs] and its value of R = 0.33, 0.5, 0.66 corresponding to the maxima recommends strongly the 1:2, 1:1 and 2:1 host to guest stoichiometry in the inclusion complexes[16]. In the present work we have found R = 0.66 suggesting 2:1 host to guest stoichiometry[17, 18]**(Scheme 2)**.

3.2 HRMS Analysis of Inclusion complexes:

Further confirmation about the formation inclusion complexes of stoichiometry 2:1 was obtained from the mass spectroscopic study of the solid inclusion complexes. After dissolving the inclusion complexes in methanol the spectra were recorded which are shown in the **Figure 2.** According to the spectra the peaks at the m/z 2226.86and 2551.97 corresponds to the $[ALVC+2\alpha\text{-}CD+H]^+$ and $[ALVC+2\beta\text{-}CD+H]^+$respectively**(Table S3)**.The appearance of the peaks in the spectra showing appreciable abundance simply implies the formation of the [ALVC+2α-CD] and [ALVC+2β-CD]inclusion complexes of 2:1 host to guest stoichiometry[19, 20](**Scheme 2**).

3.3 ^{1}H NMR and 2D ROESY NMR spectra analysis:

The mechanism of inclusion complexation with the identification of part of the guest molecule that undergoes insertion into the hydrophobic cavity of cyclodextrin was achieved and concluded by 1H NMR as well as 2D ROESY NMR spectroscopic study. Cyclodextrins having the truncated structure H3 and H5 protons are oriented inside the cavity whereas H1, H2 and H4 protons are exposed to the outer side of CDs[21](**Scheme 1**). So, the molecule that undergo insertion into the cavity must interact with H3 and H5 protons of CDs to show chemical shift in 1H NMR spectrum owing to their mutual shielding through space[22]. Encapsulation of aromatic guest molecule ring current of the aromatic moiety exerts diamagnetic shielding to the H3 and H5 protons of the CDs[23](**Table S4**). 1H NMR spectra of pure α-CD, β-CD, ALVC as well as the inclusion complexes are shown in **Figure S1-S5**respectively. From the 1H NMR spectra it was observed, there are considerable upfield shift of the H3, H5 protons of CDs and the interacting protons of the guest molecule that confirms the formation of inclusion complexes[24]**(Figure S1-S5**.)

2D ROESY NMR spectroscopy brings pivotal confirmation about the spatial closeness of the interacting protons by observing the intermolecular dipolar cross-correlations.[25,26] The protons within 0.4 nm in space may exert a rotating-frame NOE spectroscopy (ROESY) and produce off diagonal cross peak in the 2D NMR spectra of inclusion complexes.[27] Thus NOE cross peaks between interacting protons of host and guest in spectra helps us to identifying the special part of the guest molecule that undergoes encapsulation into the cavity of CDs. In this case significant correlation between aromatic protons of ALVC and the H3, H5 protons of cyclodextrin were identified in 2D ROESY spectra of inclusion complexes establishing the aromatic ring was encapsulated inside both the cyclodextrin cavities[28] (**Figure 3-4**). The H-6 protons situated in the narrower rim of cyclodextrins were found not to influenced by the inclusion processes, this may lead to the conclusion that incorporation of the guest molecule into the cavity of CDs takes place through the more favourable wider rim of CDs.[29] (**Scheme 2**).

3.4 FTIR spectroscopy:

Encapsulation of the guest molecule into the cyclodextrin cavity may lead to the shifting in vibrational frequencies of the interacting bonds of host and guest molecules. Considerable shifting in the vibrational frequencies of the interacting

bonds in the FTIR spectra of inclusion complexes compared to the frequencies of the pure ALVC and CDs suggests the formation of inclusion complexes and simultaneously, it makes us possible to identify the encapsulated part of the guest molecule as obtained from the 2D ROESY NMR spectroscopic study.[30,31] FTIR spectra of all the samples in this regard, recorded by preparing KBr disk are shown in **Figure 5** and some signals responsible for significant bond vibration are listed in **Table S5**.

Innumerable interactions of the ALVC and α-CD in the [ALVC+α-CD] inclusion complex were analysed as follows- (i) The signal at 2936.05 cm^{-1} for aromatic –C-H stretching of ALVC was found to shifted to 2925.26 cm^{-1} in the inclusion complex. (ii) the aromatic C-C stretching of ALVC was at 1397.17- 1598.11 cm^{-1}, whereas for inclusion complex it is appeared at 1402.23-1613.22 cm^{-1}. (iii) the peaks at 1024.25 cm^{-1} responsible for aromatic in plane –C-H bending for ALVC shifted to 1028.41 cm^{-1} in case of inclusion complex. (iv) the signals at 702.14-884.27 cm^{-1} appearing for aromatic out-of-plane –C-H bending were found to appear at 715.21-849.27 cm^{-1} in case of inclusion complex. This may be due to the various interaction taking place during encapsulation of ALVC. (**Figure 5**)

The shifting of the IR signals that adequately clarifies the formation of [ALVC+β-CD] inclusion complex. (i)The signal for aromatic –C-H stretching of ALVC was at 2936.05 cm^{-1} found to appear at 2927.09 cm^{-1} in the inclusion complex. (ii) the signals responsible for aromatic C-C stretching of ALVC was at 1397.17- 1598.11 cm^{-1}, but it is shifted to 1406.11-1615.12cm^{-1} for inclusion complex. (iii) the peaks at 1024.25 cm^{-1} for aromatic in plane –C-H bending for ALVC shifted to 1031.19 cm^{-1} in case of inclusion complex. (iv) the signals at 702.14-884.27 cm^{-1} appearing for aromatic out-of-plane –C-H bending were found to appear at 710.12-860.17 cm^{-1} in case of inclusion complex (**Figure 5**). Thus, FTIR spectral analysis also suggests the same outcomes as obtained from the 2D ROESY spectral analysis.

Appearance of no any other additional peaks in the FTIR spectra suggests there is no chemical reaction taking place during encapsulation and all the spectral changes happened responsible for inclusion complex formation.

3.5 XRD:

For the elucidation of various physicochemical properties of inclusion complexes, pure ALVC and CDs, X-ray diffraction data would come helpful in this case which are shown in **Figure 6**. The pure ALVC shows distinctive sharp, highly intense and less diffused diffraction peaks at angles of 2θ values of 3.85^0, 7.65^0 and 15.2^0. α-cyclodextrin registered its characteristics intense diffraction peaks at 2θ values of 5.35^0, 9.95^0, 13.65^0, 14.4^0 and 21.75^0. According to the diffractogram of β-cyclodextrin the intense peaks were recognised at the 2θ values of 4.7^0, 12.8^0, 17.15^0 and 28.8^0. Analysing the diffractogram of ALVC-α-CD inclusion complex, it was found that, all the characteristic peak of the ALVC get disappeared registering a new diffuse peak of low intensity at 2θ angle of 20.05^0. Similarly, in the case of ALVC-β-CD inclusion complex the peak position responsible for ALVC get shifted to 3.95^0, 7.4^0 and 15.65^0 respectively. Thus, disappearance of significant guest peaks, decrease of peak intensity with slight shifting of peak position and importantly, appearance of new characteristic peak in the diffractogram of inclusion complexes supports the inclusion phenomenon as discussed herewith.[32, 33, 34]

3.6 DSC thermogram:

The differential scanning calorimetry (DSC) is a very convenient technique for the exploration of thermal properties of CD based inclusion complexes because, we can gather both the qualitative and quantitative insight about the physicochemical state of the drug while encapsulated into the cavity of CDs. Generally, the shifting of an endothermic peak to a different temperature or absence of an endothermic peak for the pure guest molecule in the inclusion complexes are found in DSC thermogram which indicates a change in melting point, crystal lattice or sublimation point due to inclusion complexation[35, 36, 37, 38]. DSC thermograms of inclusion complexes and pure ALVC are depicted in **Figure 7**. From the **Figure 7** it is evident that an endothermic peak at 104.98^0C corresponding to the melting point of pure ALVC get shifted with the reduction of peak intensity to 102.80^0C and 102.84^0C for ALVC-α-CD and ALVC-β-CD inclusion complexes respectively. The intensity of the another peak at 189.86^0C get reduced drastically while going from pure ALVC to inclusion complexes. This indicates reduction of drug crystallinity through amorphization by ALVC-CDs inclusion complex formation.

3.7 Scanning Electron Microscope (SEM):

Scanning Electron Microscope (SEM) is a type of electron microscope that produces images of the sample that enable us to about the surface morphology, surface texture and particle size of solid materials[38, 39, 40, 41].The SEM images describing the surface morphology of inclusion complexes, ALVC-CDs physical mixture, pure ALVC and CDs are shown in **Figure 8**. It is evident from the analysis of the microscopic images of the inclusion complexes, ALVC-CDs physical mixture, pure ALVC and CDs, the surface morphologies are different from each of the categories. The may be possibly for the formation of inclusion complexes. Thus, it appears to an additional evidence about the formation of inclusion complexes along with 2D ROESY NMR analysis.

3.8 UV and solubility:

Well-known Higuchi and Connor method was employed to study the phase solubility of the ALVC in CDs[38, 42, 43]. A set of aqueous solution of CDs were prepared separately in the concentration range 0 to 10 mM. The pH of the prepared solutions was maintained to 7.4 using phosphate buffer solution. An excess amount of ALVC were added to each of the solutions of set prepared previously with CDs. The solutions were then allowed to stir for 24 hours at 25^0C on a magnetic stirrer. Then, the solutions were filtered and diluted properly to determine the amount of contained ALVC through dissolution in the solution UV-vis spectroscopically using 1 cm quartz cuvette. Apparent water solubilities were measured by plotting a solubility curve as a function of CDs concentration **(Figure S6-S7)**. The amount of ALVC contained by the solution are shown in **Table 1**.

We also calculated the association constant (K_a) using the following equation-

$$K_a = \frac{Slope}{S_0(1-Slope)} \qquad (1)$$

Where, S_0 represents the inherent water solubility of ALVC in water and the Slope is according to the slope of the phase solubility plot. With the known value of K_a, the complexation efficiency (CE) was determined as follows-

$$CE = \frac{Slope}{1-Slope} = K_a \times S_0 \qquad (2)$$

Where, K_a, S_0 and slope represents the same as mentioned above. The association constants (K_a) of the inclusion complexes and complexation efficiencies (CE) are listed in **Table 2**. The enhancement of solubility thus simply suggests the formation of inclusion complexes[44].

3.9 Ultraviolet Spectroscopy: The association constants (Ka) of the Inclusion Complexes:

The capability of the Guest to bind into the Host's hydrophobic cavity and the association constants (Ka) representing the extent of stability of the ICs were calculated using the Benesi-Hildebrand equation[41, 45, 46]. The UV-vis spectroscopic data were used to determine the association constant (Ka) of the ICs in the solution phase.[47] As the molar extinction coefficient (Δε) depends upon the solvent polarity, the absorbance of the guest molecule must change while going from polar aqueous media to the apolar hydrophobic cavity of the CDs to form ICs.[48,49] The data obtainable from the UV-vis spectroscopic measurement are listed in the **Table S6-S7**. The Benesi-Hildebrand method uses the following equation[45, 47, 50, 51]to determine the association constant of the ICs.

$$\frac{1}{\Delta A} = \frac{1}{\Delta\varepsilon[DGs]K_a}\frac{1}{[CD]^n} + \frac{1}{\Delta\varepsilon[DGs]} \qquad (3)$$

Where, ΔA is the difference in absorbances of ALVC without CDs and with the CDs. [DGs] represents the concentration of ALVC. The value of (n) says about the stoichiometry of the ICs. When the linearity of the double reciprocal plot fits by putting n=1 in the above equation then it suggests 1:1 stoichiometry of the ICs. But, when n=2 suggests the 2:1 inclusion complex of the Host to the Guest. Here, we observed no linear relationship of the Benesi-Hildebrand double reciprocal plot indicating the composition of complex was not 1:1. On the other hand the linearity of the plot best fits when n=2 suggesting the 2:1 stoichiometry of the ICs[15] as obtained from the Job's plot.

$$\frac{1}{\Delta A} = \frac{1}{\Delta\varepsilon[DGs]K_a}\frac{1}{[CD]^2} + \frac{1}{\Delta\varepsilon[DGs]} \qquad (4)$$

The value of slope and intercept of the double reciprocal plot **(Figure S7-S8)** enable us to calculate the association constants (K_a) of the inclusion complexes and listed in the T**able 3**.

With knowledge of the association constants (K_a) of the ICs at various temperature the thermodynamic parameters of the ICs were calculated using the Van't Hoff equation-

$$\ln K_a = -\frac{\Delta H^0}{RT} + \frac{\Delta S^0}{R} \qquad (5)$$

The thermodynamic parameters of the formation of ICs obtained from a linear plot **(Figure S9)** of Van't Hoff equation, listed in the **Table 3** it was found that, enthalpy change of formation is negative and entropy increases while formation of ICs, suggesting an exothermic and entropically driven process making the process spontaneous which is reflected from the free energy change of the process.

3.10 Fluorescence and binding of Guest to HSA:

The ALVC-HSA interaction and the quenching in fluorescence intensity caused by the changes in the environment surrounding ALVC. The fluorescence spectra were recorded at a fixed concentration of HSA exciting at 295 nm. Fluorescence spectra of HSA were recorded for a set of solutions containing varying amount of ALVC in the solutions and results were fed to Stern-Volmer equation[52] to calculate the binding constant of the ALVC to HSA.

$$F_0/F = 1 + K_{sv}[Q] = 1 + K_q\tau_0[Q] \qquad (6)$$

Where, F_0 and F represents the fluorescence intensities of HSA in the absence and presence of ALVC respectively, K_{sv} is the linear Stern Volmer constant and [Q] is the concentration of ALVC i.e. the concentration of the quencher. The Stern-Volmer quenching constant (K_{sv}), is the measure of efficiency of quenching. K_q indicates the bimolecular quenching rate constant and τ_0 represents the average fluorescent life time of protein without quencher, which is 5.6×10^{-9}s[53]. The value of binding constant was calculated using the following logarithm equation,

$$\log[(F_0 - F/F)] = \log K_b + n\log[Q] \qquad (7)$$

Where, F_0 and F represents the fluorescence intensities of the HSA in the absence and presence of different concentration of ALVC and n is the number of binding sites. The values of binding constant (Kb) obtained from the slope of the linear plot[54] **(Figure 9)** of $\log(F\text{-}F_0)/F$ versus log[Q] and are listed in the **Table 4**.

4. Conclusions:

All the experiments suggest the successful formation of inclusion complex with 2:1 stoichiometry. The association constants of the inclusion complexes of ALVC formed with β-cyclodextrin were found greater than that of the inclusion complexes formed with the α-cyclodextrin and hence more stable, this is may be due to the better fitness of the guest molecule into the larger hydrophobic cavity of β-cyclodextrin compared to the α-cyclodextrin. The ready availability of the association constants enables us to calculate the thermodynamic parameters of the inclusion process which makes the thermodynamic background of the process and recognise it as a thermodynamically feasible process. When the guest molecule gets encapsulated into the hydrophobic cavity of cyclodextrin molecule, the water molecules removed from the hydrophobic cavity of cyclodextrin molecule increases the entropy of the process. Thus, the hydrophobic-hydrophobic interaction and entropy factor would become the driving forces for the formation of inclusion complexes. The binding constant of ALVC to the HSA become appreciable showing an affinity of HSA towards the drug molecule. Thus, it is expected that, the drug molecule gets released from the inclusion complex and binds successfully with the HSA which then get transported to the targeted site promoting regulatory release consequently reduces overdoses without any chemical modification.

Conflicts of interest: There is no conflicts of interest.

Acknowledgements: Prof. M. N. Roy would like to acknowledge UGC, New Delhi, Government of India, for being awarded One Time Grant under Basic Scientific Research via the grant-in-Aid no. F.4-10/2010 (BSR). BR is thankful to the "State

Fellowship" bearing reference No. 1743/R-2017 dated 18.04.2017 and Mr. Goutam Sarkar, The H.O.D., USIC, University of North Bengal, Darjeeling is also highly acknowledged for executing SEM associated with this paper and his sincere co-operation.

TABLES

Table 1: The association constant (K_a) and complexation efficiency of the inclusion complexes at 298.15 K.

Guest	Host	Temperature (K[a])	K_a (×10^{-3})	CE
ALVC	α– CD	298.15	861.43	2.58
	β – CD	298.15	871.75	2.62

Table 2: The solubility of ALVC (moles/litre) in the aqueous solution of cyclodextrins of concentration ranging from 0.002 to 0.01 (M).

α-CD (M)	Solubility of ALVC (moles/litre)	β-CD (M)	Solubility of ALVC (moles/litre)
0.002	0.0166	0.002	0.0179
0.004	0.0218	0.004	0.0221
0.006	0.0250	0.006	0.0259
0.008	0.0276	0.008	0.0282
0.01	0.0300	0.01	0.0310

Table 3. Association Constant obtained from Benesi-Hildebrand method (K_a) using the UV-vis spectroscopic data at 293.15 to 303.15 K and the thermodynamic parameters calculated using Van't Hoff equation.

Guest	Host	Temperature (K[a])	K_a (×10^{-6}) /M^{-2}	ΔH^0 (KJ mol^{-1})	ΔS^0 (J mol^{-1} K^{-1})	ΔG^0 (KJ mol^{-1})
ALVC	α– CD	293.15	919	-8.16	143.71	-51.01
		298.15	856			
		303.15	823			
	β – CD	293.15	921	-7.85	144.85	-51.04
		298.15	877			
		303.15	829			

[a]Standard uncertainty in temperature, u, are u(T) = ± 0.01 K

Table 4: HSA-ALVC binding constant and number of binding site.

Binding constant (K_b)×10^{-3}/M^{-1}	Number of binding site
1.03	0.86

Table S1. UV-Vis spectroscopic data for the generation of Job plots of aqueous ALVC+α-CD system at 298.15 K[a].

ALVC + ALPHA - CYCLODEXTRIN							
ALVC (mL)	α-CD (mL)	ALVC (μM)	α-CD (μM)	$\frac{[\mathbf{ALVC}]}{[\mathbf{ALVC}]+[\alpha-\mathbf{CD}]}$	Absorbance (A)	ΔA	$\frac{\Delta\mathbf{A}\times[\mathbf{ALVC}]}{[\boldsymbol{ALVC}]+[\alpha-\mathbf{CD}]}$
0	3	0	100	0	0.0087	0.0598	0.0000
0.3	2.7	10	90	0.1	0.0390	0.0295	0.0030
0.6	2.4	20	80	0.2	0.0401	0.0284	0.0057
0.9	2.1	30	70	0.3	0.0441	0.0245	0.0073
1.2	1.8	40	60	0.4	0.0456	0.0229	0.0092
1.5	1.5	50	50	0.5	0.0447	0.0238	0.0119
1.8	1.2	60	40	0.6	0.0451	0.0234	0.0141
2.1	0.9	70	30	0.7	0.0501	0.0185	0.0129
2.4	0.6	80	20	0.8	0.0544	0.0141	0.0113
2.7	0.3	90	10	0.9	0.0635	0.0050	0.0045
3	0	100	0	1	0.0685	0.0000	0.0000

Table S2. UV-Vis spectroscopic data for the generation of Job plots of aqueous ALVC+β-CD system at 298.15 K[a].

ALVC + BETA - CYCLODEXTRIN							
ALVC (mL)	β-CD (mL)	ALVC (μM)	β-CD (μM)	$\frac{[ALVC]}{[ALVC]+[\beta-CD]}$	Absorbance (A)	ΔA	$\frac{\Delta A \times [ALVC]}{[ALVC]+[\beta-CD]}$
0	3	0	100	0	0.0091	0.0607	0.0000
0.3	2.7	10	90	0.1	0.0385	0.0313	0.0031
0.6	2.4	20	80	0.2	0.0336	0.0362	0.0072
0.9	2.1	30	70	0.3	0.0431	0.0267	0.0080
1.2	1.8	40	60	0.4	0.0459	0.0239	0.0096
1.5	1.5	50	50	0.5	0.0472	0.0226	0.0113
1.8	1.2	60	40	0.6	0.0466	0.0232	0.0139
2.1	0.9	70	30	0.7	0.0518	0.0181	0.0126
2.4	0.6	80	20	0.8	0.0567	0.0131	0.0105
2.7	0.3	90	10	0.9	0.0648	0.0050	0.0045
3	0	100	0	1	0.0698	0.0000	0.0000

Table S3. Mass spectrometric data showing the molecular ion peak corresponding to the 2:1 Host –Guest inclusion complexes.

ALVC+α-CD inclusion complex (IC_1)		ALVC+β-CD inclusion complex (IC_2)	
m/z	Ion	m/z	Ion
2226.86	$[ALVC+ 2\ \alpha\text{-CD}]^+$	2551.97	$[ALVC+ 2\ \beta\text{-CD}]^+$

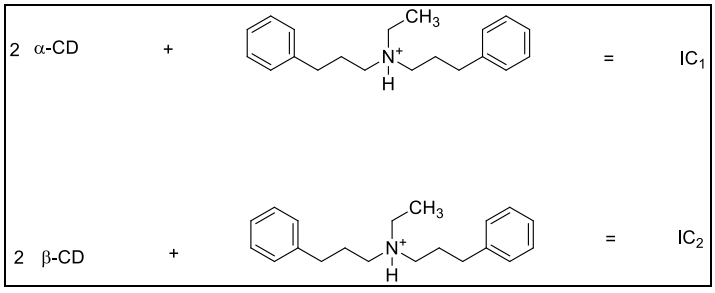

Table S4. ^{1}H NMR data of the pure α-Cyclodextrin, β-Cyclodextrin, alverine citrate and the solid inclusion complexes.

α-Cyclodextrin (400 MHz, Solvent: D2O), δ/ppm	**β-Cyclodextrin (400 MHz, Solvent: D2O), δ/ppm**
3.43 (6H, t, J = 8 Hz), 3.50 (6H, dd, J = 3.00, 10.00 Hz), 3.73 (18H, m), 3.84 (6H, t, J = 8Hz), 4.91 (6H, d, J = 4.00 Hz)	3.44 (7H, t, J = 8.00 Hz), 3.50 (7H, dd, J = 8 Hz, 4 Hz), 3.72 (21H, m), 3.82 (7H, t, J = 8 Hz), 4.92 (7H, d, J = 4 Hz)
Alverine citrate (400 MHz, Solvent: D2O), δ/ppm)	
1.04 (3H, t), 1.77 (4H, m), 2.53 (4H, m), 2.67 (4H, t), 2.92 (4H, t), 3.01 (2H, q), 7.18 (10H, m)	
ALVC+α-CD inclusion complex (400 MHz, Solvent: D2O), δ/ppm)	**ALVC+β-CD inclusion complex (400 MHz, Solvent: D2O), δ/ppm)**
1.04 (3H, t), 1.78 (4H, m), 2.54 (4H, t), 2.68 (4H, t), 2.92 (4H, t), 3.02 (2H, q), 3.42 (6H, t), 3.49 (6H, dd), 3.72 (18H, m), 3.79 (6H, d), 7.19 (10H, m)	1.03 (3H, t), 1.74 (4H, m), 2.53 (4H, t), 2.67 (4H, t), 2.92 (4H, t), 3.01 (2H, q), 3.44 (7H, t), 3.56 (7H, dd), 3.70 (21H, m), 7.16 (10H, m)

Table S5. Frequencies at FTIR spectra of α-CD, β-CD, 18-Crown-6, ALVC and solid inclusion complexes.

α-cyclodextrin (α-CD)		**β-cyclodextrin (β-CD)**	
Wavenumber (cm^{-1})	**Group**	**Wavenumber (cm^{-1})**	**Group**
3408.25	-O-H stretching	3370.21	-O-H stretching
2932.12	-C-H stretching	2916.35	-C-H stretching
1406.17	-C-H and -O-H bending	1412.27	-C-H and -O-H bending
1154.26	C-O-C bending	1158.14	C-O-C bending
1030.19	C-C-O stretching	1026.52	C-C-O stretching
978.23	skeletal vibration involving α-1,4linkage	938.08	skeletal vibration involving α-1,4linkage

Alverine citrate (ALVC)			
Wavenumber (cm^{-1})		**Group**	
3396.45		-O-H stretching/N-H stretching	
2806.31		-C-H stretching	
1602.37		C=C stretching	
1458.51		-C-H bending (methyl/methylene)	
1272.59		-C-O stretching (phenol)	
1172.23		-C-N stretching	
1070.13		-C-O stretching (secondary alcohol)	
792.26		Aromatic -C-H out-of-plane bending	
700.15		Aromatic -C-H out-of-plane bending	
ALVC+α-CD		**ALVC+β-CD**	
Wavenumber (cm^{-1})	**Group**	**Wavenumber (cm^{-1})**	**Group**
3374.08	-O-H stretching/N-H stretching	3320.19	-O-H stretching/N-H stretching
2929.29	-C-H stretching	2932.18	-C-H stretching
1628.35	C=C stretching	1604.08	C=C stretching
1333.45	-C-N stretching	1336.35	-C-N stretching
1154.27	-C-O stretching (phenol)	1158.08	-C-O stretching (phenol)
1030.23	-C-O stretching (secondary alcohol)	1032.29	-C-O stretching (secondary alcohol)
707.25	Aromatic -C-H out-of-plane bending	754.36	Aromatic -C-H out-of-plane bending
583.26	Aromatic -C-H out-of-plane bending	582.13	Aromatic -C-H out-of-plane bending

Table S6. UV-vis spectroscopic data for the Benesi-Hildebrand double reciprocal plot of (ALVC+α-CD) system at 293.15 to 303.15 K[a].

Temp (K[a])	ALVC (μM)	α-CD (μM)	Ao	A	ΔA	1/[α-CD]^2 (M^{-2})	1/ΔA	Intercept	Slope	Ka ($M^{-2}\times10^{-6}$)
293.15	80	20	0.0614	0.0923	0.0309	0.0025	32.3948	8.7231	9494.8	919
	80	50		0.1409	0.0795	0.0004	12.5798			
	80	80		0.1464	0.0850	0.0002	11.7659			
	80	110		0.1759	0.1145	0.0001	8.7374			
	80	140		0.1801	0.1187	0.0001	8.4254			
298.15	80	20	0.0624	0.0929	0.0305	0.0025	32.8201	8.3936	9806.9	856
	80	50		0.1405	0.0781	0.0004	12.8053			
	80	80		0.1570	0.0946	0.0002	10.5718			
	80	110		0.1775	0.1151	0.0001	8.6918			
	80	140		0.1820	0.1196	0.0001	8.3620			
303.15	80	20	0.0631	0.0934	0.0303	0.0025	33.0369	8.1871	9951.3	823
	80	50		0.1449	0.0818	0.0004	12.2261			
	80	80		0.1604	0.0973	0.0002	10.2784			
	80	110		0.1771	0.1140	0.0001	8.7757			
	80	140		0.1827	0.1196	0.0001	8.3620			

Table S7. UV-vis spectroscopic data for the Benesi-Hildebrand double reciprocal plot of (ALVC+β-CD) system at 293.15 to 303.15 K[a].

Temp (K[a])	ALVC (μM)	β-CD (μM)	Ao	A	ΔA	1/[β-CD]^2 (M^{-2})	1/ΔA	Intercept	Slope	Ka ($M^{-2}\times10^{-6}$)
293.15	80	20	0.0616	0.0930	0.0301	0.0025	33.2566	8.7447	9485.1	921
	80	50		0.1416	0.0787	0.0004	12.7077			
	80	80		0.1471	0.0842	0.0002	11.8777			
	80	110		0.1756	0.1127	0.0001	8.8770			
	80	140		0.1808	0.1179	0.0001	8.4826			
298.15	80	20	0.0621	0.0943	0.0322	0.0025	31.0374	8.0806	9211.3	877
	80	50		0.1429	0.0808	0.0004	12.3774			
	80	80		0.1714	0.1093	0.0002	9.1499			
	80	110		0.1752	0.1131	0.0001	8.8456			
	80	140		0.1815	0.1194	0.0001	8.3760			
303.15	80	20	0.0627	0.0949	0.0322	0.0025	31.0857	7.7624	9367.3	829
	80	50		0.1441	0.0814	0.0004	12.2861			
	80	80		0.1766	0.1139	0.0002	8.7803			
	80	110		0.1764	0.1137	0.0001	8.7989			
	80	140		0.1919	0.1292	0.0001	7.7418			

Table S8. Data of the van't Hoff equation for calculation of thermodynamic parameters ΔH^o, ΔS^o and ΔG^0 of different (ALVC+α-CD) and (ALVC+β-CD) inclusion complexes.

HOST	T (K[a])	1/T	Ka ($M^{-2}\times10^{-6}$)	lnKa	Slope	Intercept	ΔH^0 (KJ mol^{-1})	ΔS^0 (J mol^{-1} K^{-1})	ΔG^0 (KJ mol^{-1})
	293.15	0.00341	919	20.6388					
α-CD	298.15	0.00335	856	20.5678	981.97	17.284	-8.16	143.71	-51.01
	303.15	0.00330	823	20.5285					
	293.15	0.00341	921	20.6421					
β-CD	298.15	0.00335	877	20.5920	944.50	17.241	-7.85	144.85	-51.04
	303.15	0.00330	829	20.5357					

FIGURES

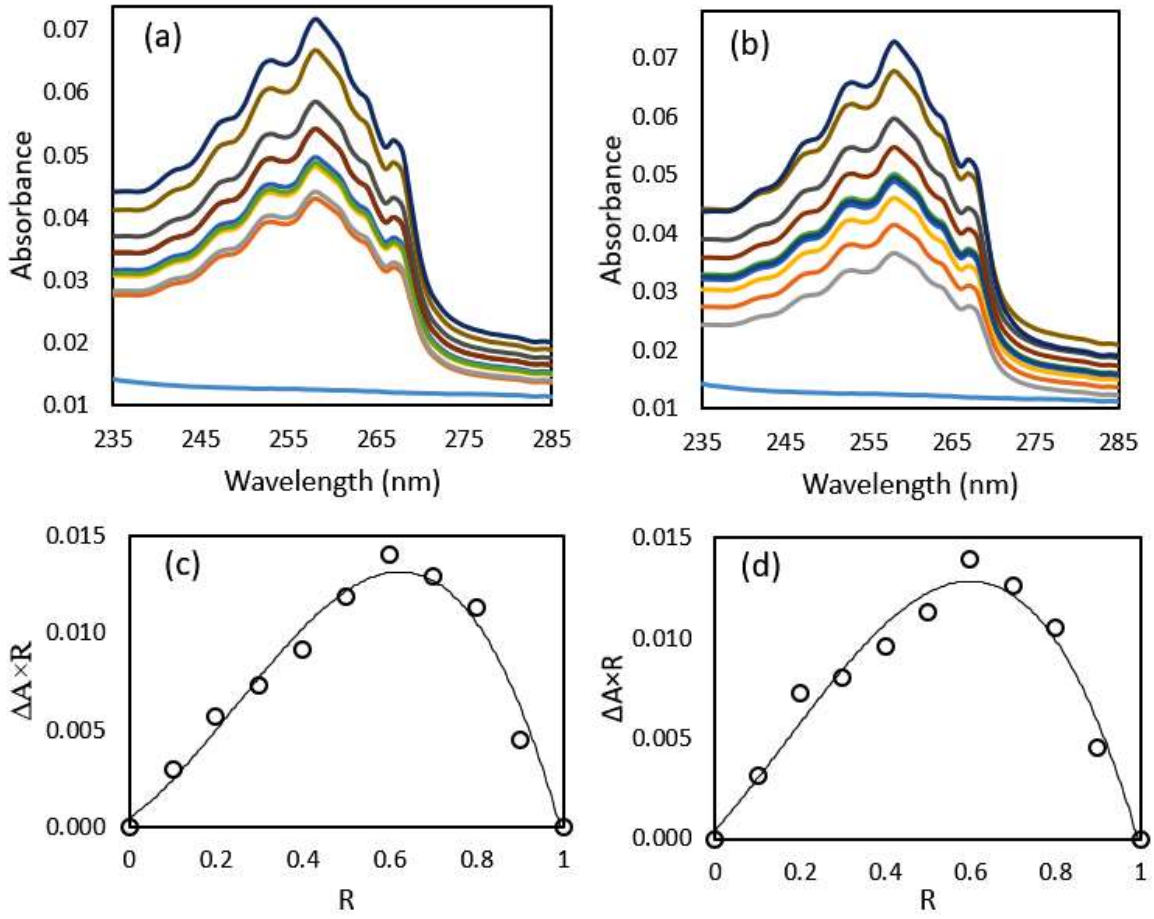

Figure 1: UV-vis spectra for the generation of Job's plot (a,c) ALVC-α-CD inclusion complexes and (b,d) ALVC-β-CD inclusion complexes.

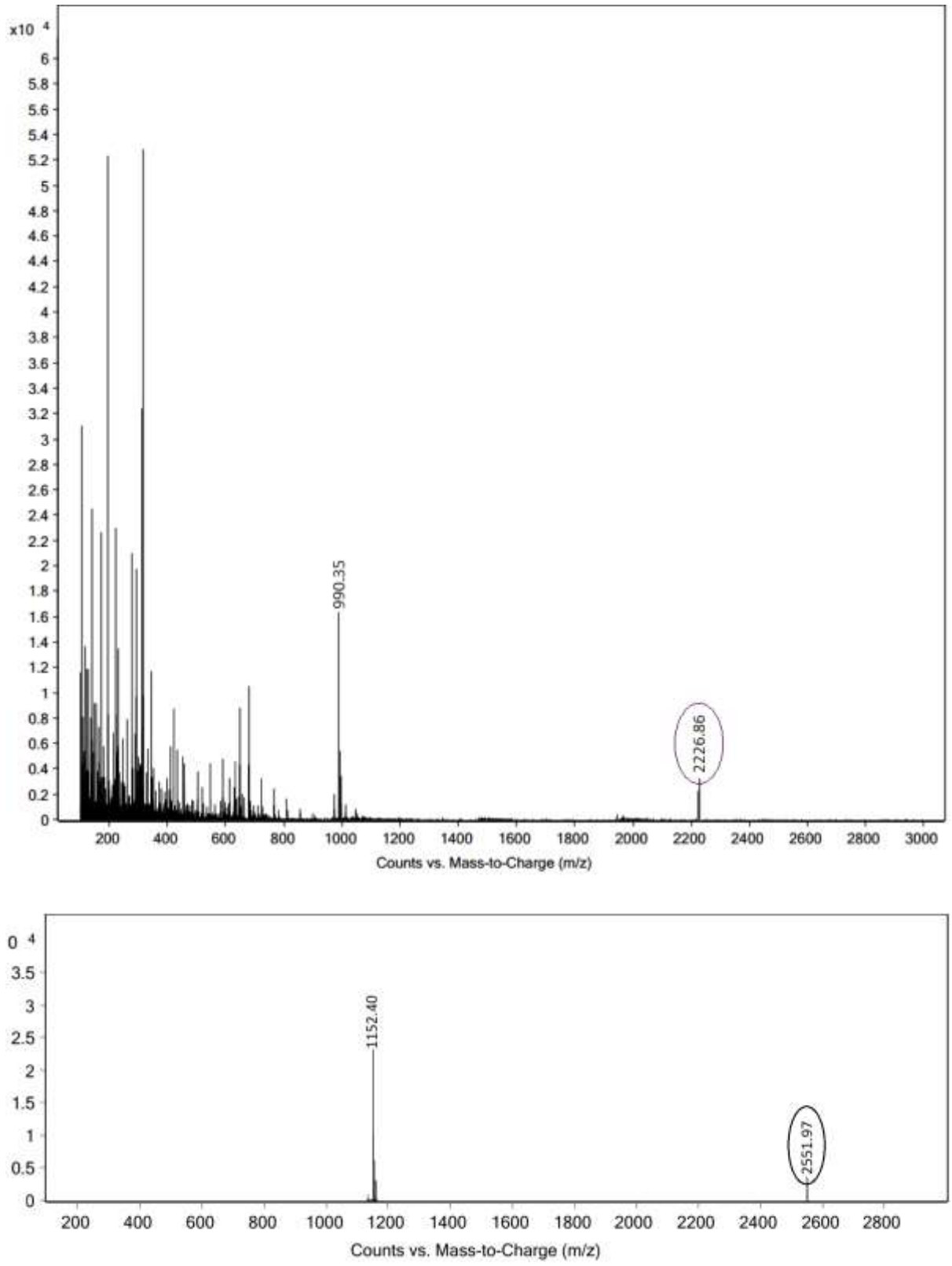

Figure 2: Mass spectra of (a) ALVC/α-CD inclusion complex, (b) ALVC/β-CD inclusion complex.

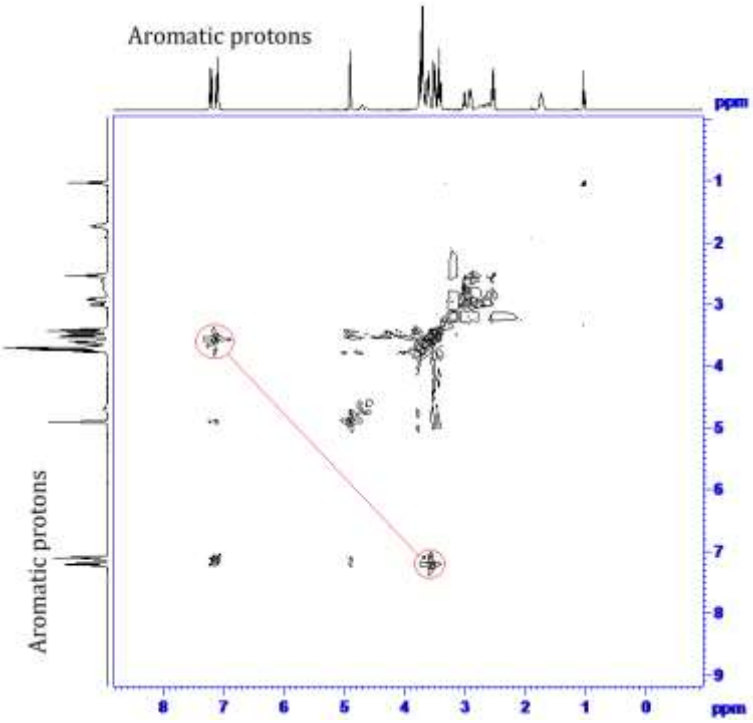

Figure 3: 2D ROESY NMR spectra of ALVC/α-CD inclusion complex.

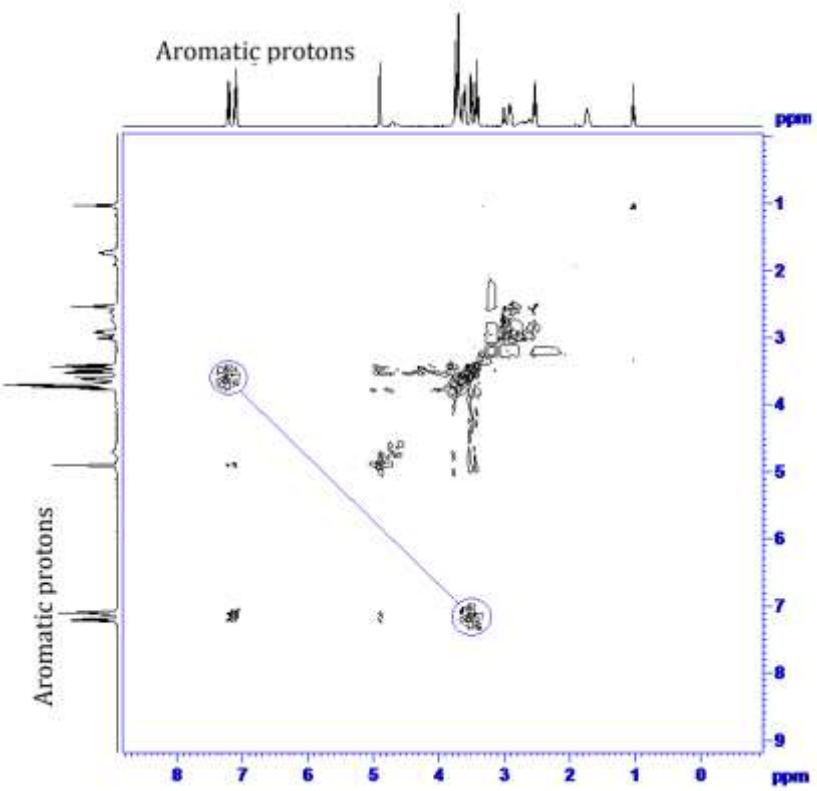

Figure 4: 2D ROESY NMR spectra of ALVC/β-CD inclusion complex.

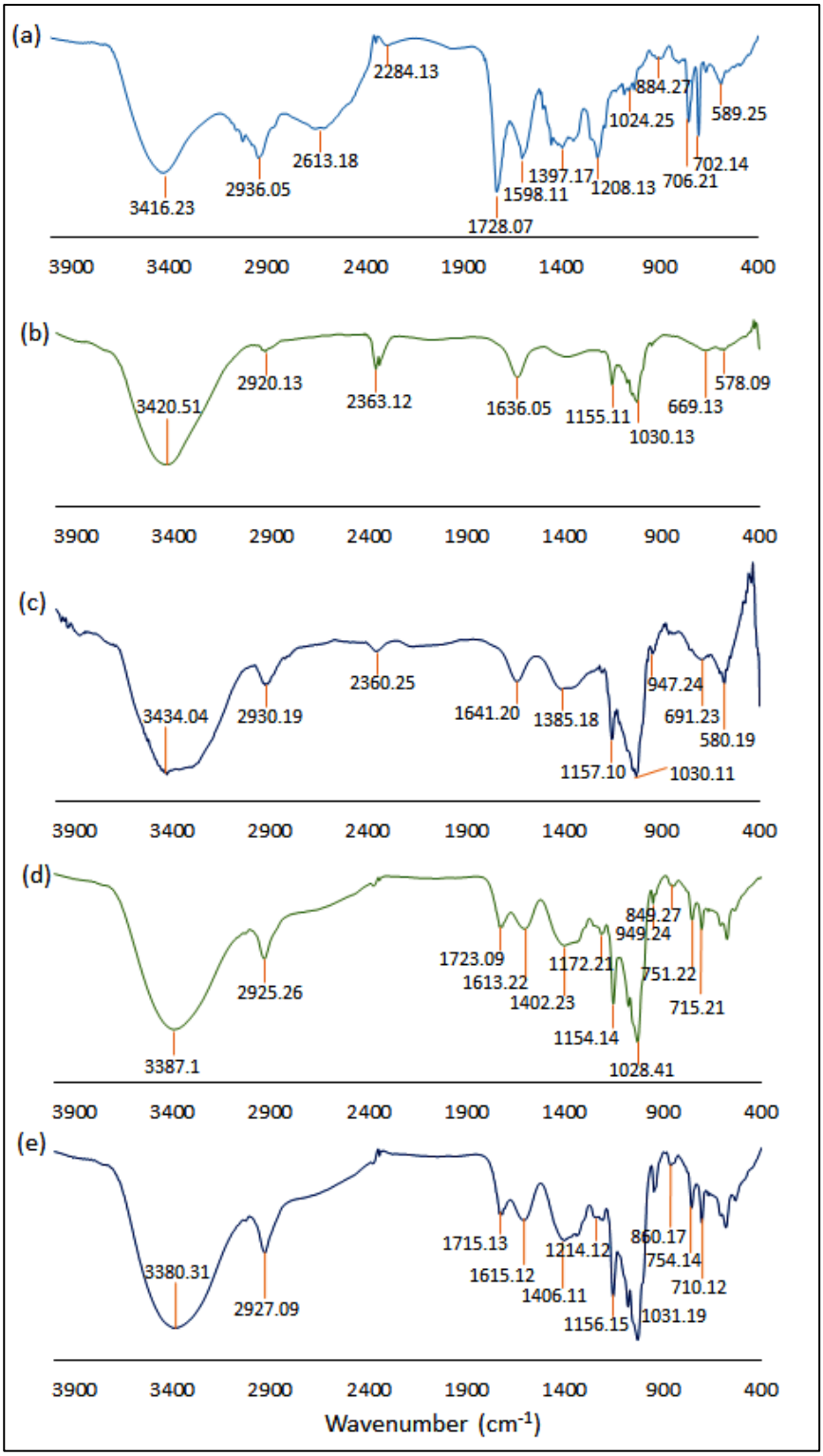

Figure 5(a, b, c, d, e): IR frequencies of (a) ALVC, (b) α-CD, (c) β-CD, (d) ALVC/α-CD inclusion complex, (e) ALVC/β-CD inclusion complex.

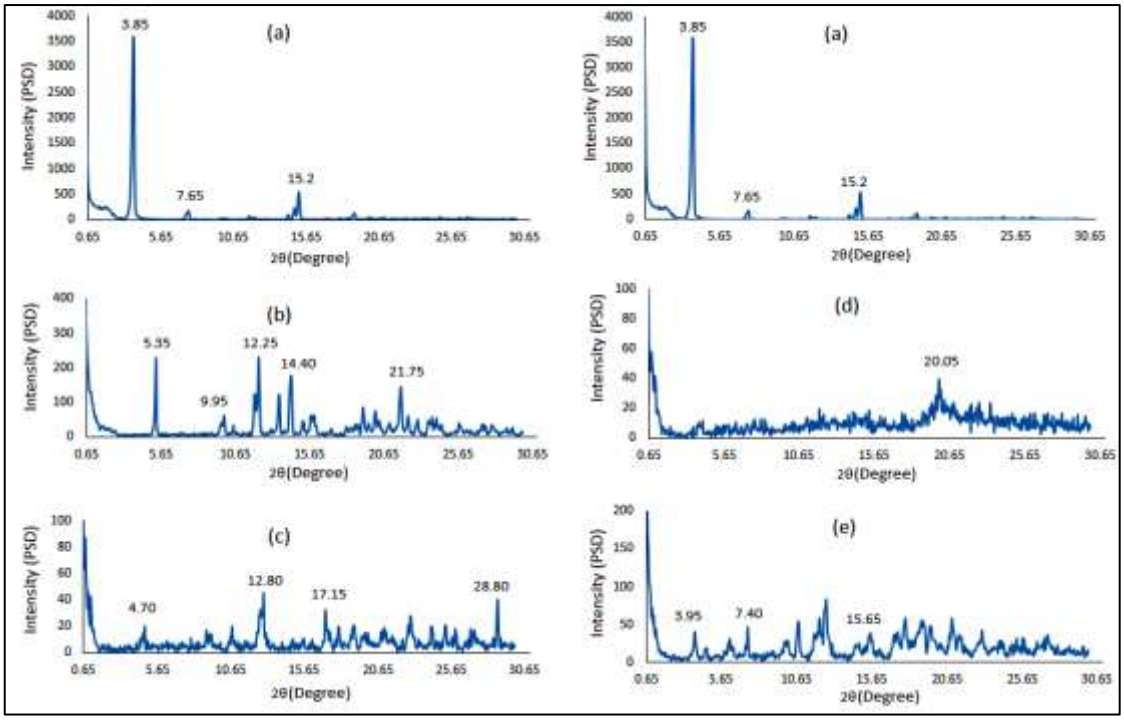

Figure 6(a, b, c, d, e): PXRD spectra of (a) ALVC, (b) α-CD, (c) β-CD, (d) ALVC/α-CD inclusion complex, (e) ALVC/β-CD inclusion complex.

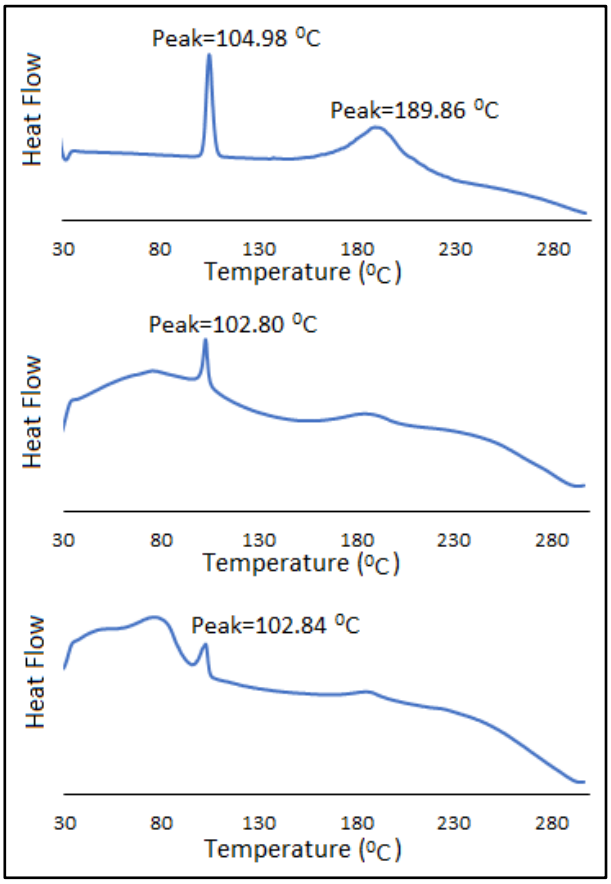

Figure 7(a, b, c): DSC thermogram of the (a) ALVC, (b) ALVC/α-CD inclusion complex, (c) ALVC/β-CD inclusion complex.

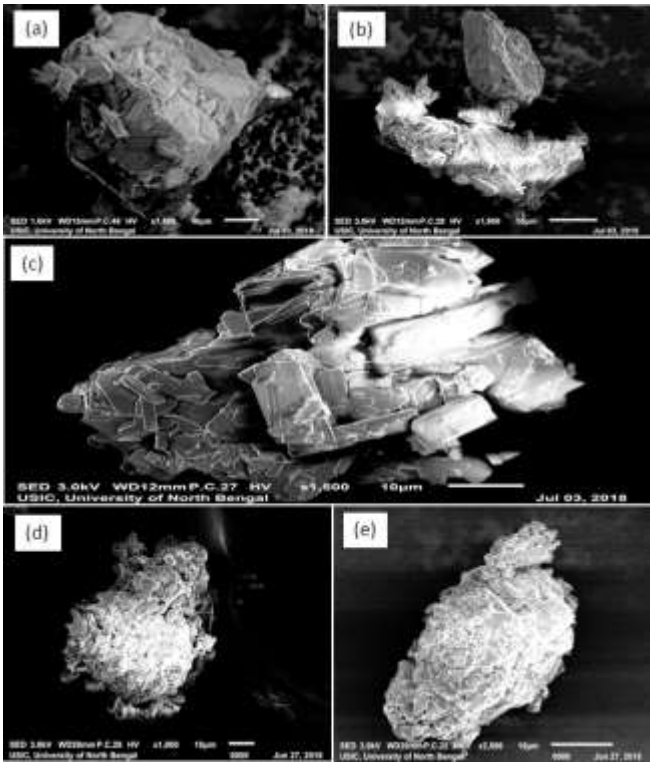

Figure 8(a, b, c, d, e): SEM images of (a) α-CD, (b) β-CD, (c) ALVC, (d) ALVC/ α-CD inclusion complex, (e) ALVC/ β-CD inclusion complex.

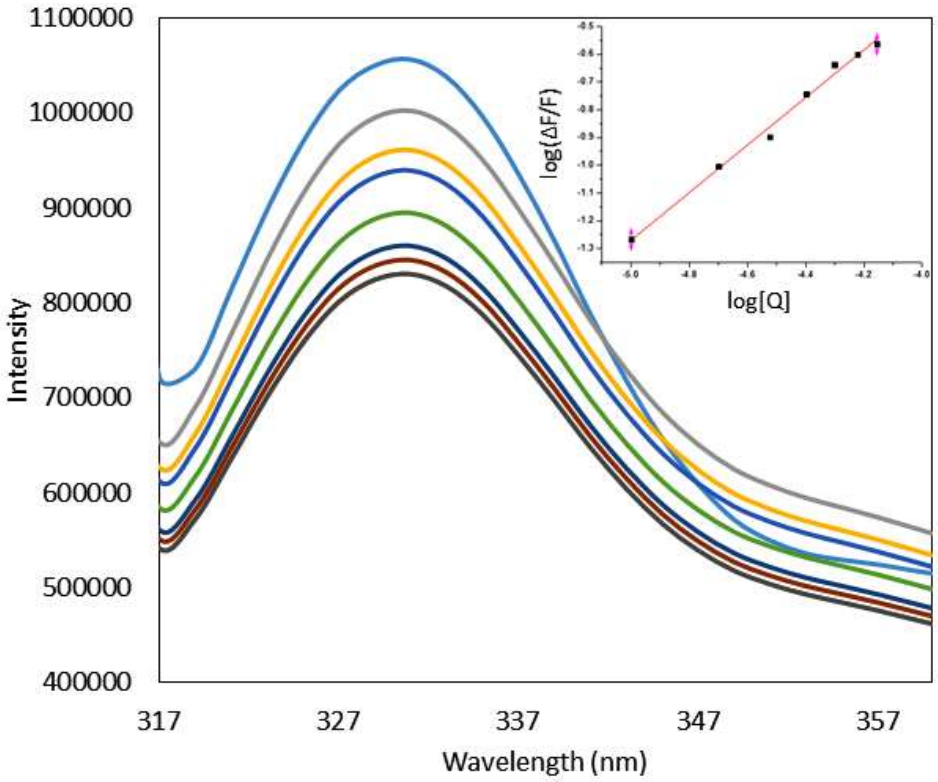

Figure 9: Fluorescence spectra and plot for obtaining binding constant.

SCHEMES

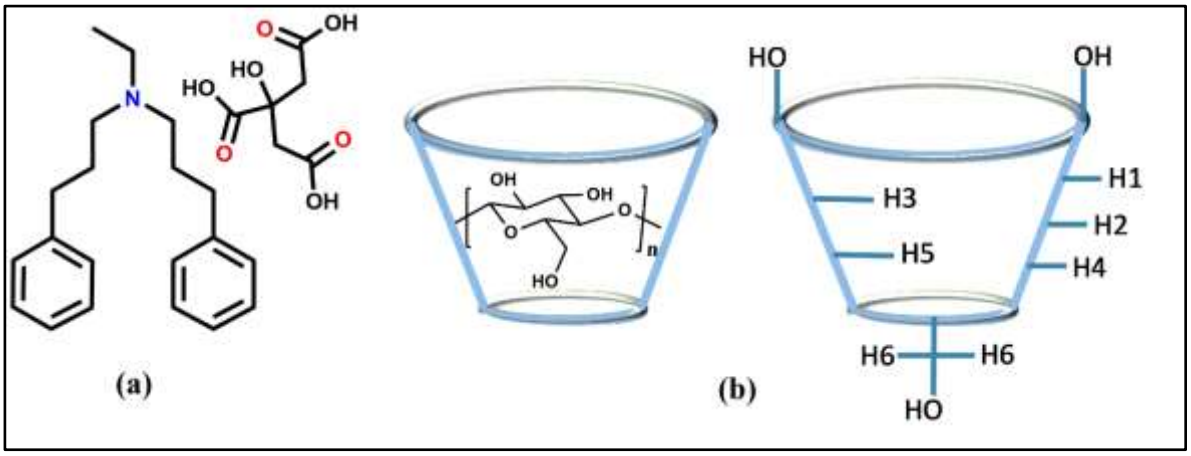

Scheme 1: Molecular structure of (a) alverine citrate, (b) α, β-cyclodextrins where, n=5 to 6 respectively.

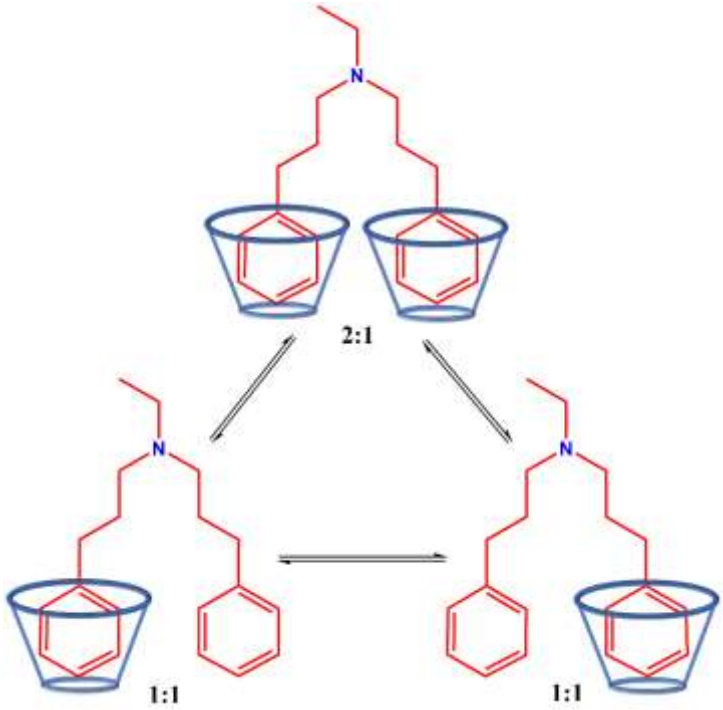

Scheme 2: Schematic representation of the formation of Inclusion Complex.